

PERFORMANCE PREDICTION OF TWIN-ENTRY TURBOCHARGER TURBINES*

S. GHASSEMI**, E. SHIRANI¹ AND A. HAJILOUY-BENISI²

¹Dept. of Mechanical Engineering, Isfahan University of Technology, Isfahan, I. R. of Iran

² Dept. of Mechanical Engineering, Sharif University of Technology, Tehran, I. R. of Iran
Email: sghassemi@gmail.com

Abstract– In this paper, the performance of the twin-entry radial flow turbine under steady state and partial admission conditions is modeled. The method, which is developed here, is based on one-dimensional performance prediction. In one-dimensional modeling, the flow properties are assumed constant on a plane normal to the flow direction. This assumption is in contrast with the flow at the rotor entry of a twin-entry turbine under partial admission condition. In this study the one-dimensional performance prediction method for a single-entry turbine is modified to analyze the twin-entry turbine. In particular, the loss coefficients due to friction, clearance and blade loading, which are already developed for single-entry turbines, are modified. Also, additional losses in the rotor are considered because of twin-entry rotor inlet conditions and the rotor-mixing losses. Indeed, in a single-entry turbine with symmetric volute, the flow tends to move toward the shroud. A correlation for the radial velocity profile at the rotor entry for this case is obtained and is considered to be optimum. Then the rotor mixing loss is estimated. Finally a model based on the above mentioned matters is developed. The results obtained from the model are compared with the experimental results and good agreements are obtained. In this paper, special behaviors of the flow in the twin-entry turbine are also investigated and some physical interpretations are presented.

Keywords – Turbocharger, radial flow, turbine, twin-entry, one-dimensional modeling, performance prediction

1. INTRODUCTION

Turbochargers are one of the most important components of the diesel engines. They increase the power output to the engine weight ratio and the efficiency. Using twin-entry radial flow turbines in turbocharging systems of small diesels gives the possibility of using the energy of pulsating exhaust gases, and is a very common practice. Despite its importance, there are not many research activities in the area of twin-entry turbocharger turbines. Almost all of the research in this area are experimental [1-4]. The researchers commonly stated that the shroud and hub side entries have different effects on the turbine performance. The best efficiency is obtained when the mass flow rate in the shroud side entry is more than the hub side entry [2-4]. Different values of the optimum mass flow ratio are given by different authors. For example, Capobianco and Gambarotta [3] gave 0.014 and Baines and Yeo [4] gave 0.6. The large difference between these values may be due to the different shape of the turbine casing they used. Capobianco and Gambarotta [3] used a turbine with inclined volute and unequal entry areas, but Baines and Yeo [4] used a turbine with a symmetric volute. It is worth mentioning that the minimum efficiency is obtained when one of the entries, in particular the shroud side, is fully closed [2-4]. The efficiency of the twin-entry turbine at full admission condition is about 7 percent less than the single entry turbine with same rotor [3].

The solution methods for the flow in the radial flow turbines can be classified as numerical and modeling. The two or three-dimensional solutions are obtained numerically. In this procedure, the researcher must be an expert in numerical methods and do not need to model the flow characteristics. But in one dimensional flow modeling, the modelers must have a good insight of the flow. In this procedure, different losses are identified and each one is modeled separately. The one-dimensional approach is used for the preliminary design procedure and is simpler and easier to use.

*Received by the editors November 13, 2002 and in final revised form November 20, 2004

**Corresponding author

56 The only numerical flow simulation obtained for this flow, as far as the authors know, is the work of
57 Lymberopoulos *et al.* [5]. They simulated the flow in the volute of a twin-entry turbine by solving the quasi
58 three-dimensional Euler equations.

59 The one-dimensional modeling of the single-entry radial turbines has been studied by many authors [6-
60 12]. However, modeling of the twin-entry turbines has not been the center of the researchers' attention. The
61 majority of the 1-D analysis is for single-entry turbines. Despite the fact that twin-entry turbines are used
62 extensively in industries, to the extent of the authors' knowledge, there has not been any paper in the
63 literature which deals with the 1-D analysis of two-entry turbines. Also, there are very few discussions about
64 the flow behavior and loss effects in these turbines. Baines and Yeo [4] explained the efficiency
65 characteristics of the turbine based on the flow patterns in the rotor. They stated that under a partial
66 admission condition, when the relative flow angle is not at its optimum value, an unsuitable inflow angle at
67 the rotor hub side results in higher losses. Although this analysis is interesting, it is not sufficient. For
68 example, this analysis cannot explain why the best efficiency is obtained when the mass flow rate of the
69 shroud side entry is more than that of the hub side entry. Another problem is that the available one-
70 dimensional flow equations are obtained only for single-entry turbines and they cannot be used for twin-
71 entry turbines directly.

72 The aims of this paper are 1) to give explanations for some of the behaviors of the turbine which have
73 not been discussed in the literature. These explanations help the extension of 1-D modeling to twin-entry
74 turbines by using more information about the flow and the losses inside the turbine, 2) to develop 1-D
75 modeling for a twin-entry turbine using similar models for a single-entry turbine. Since the coefficients in
76 the model are generally obtained from the experimental data, to accurately calculate the coefficients of the
77 model, it can be improved by using more experimental data, as they will be available in the future.

78 2. FLOW PATTERN IN THE TURBINE

79 a) Flow in the casing

80 Figure 1 shows the flow velocity, the flow angle and the incidence angle at the rotor entry (volute exit), for
81 different partial admission conditions, based on the measurements obtained by Baines and Yeo [4]. The total
82 mass flow rate is held constant at all cases. According to these experimental results, except when one of the
83 entries is fully closed, as the mass flow rate increases at one entry, the flow velocity also increases at the
84 same passage, and the flow angle does not change much at this section. Based on Whitfield and Baines [11],
85 simple considerations of angular momentum, the angle of flow leaving a vaneless volute is a function of
86 geometry only. But this situation does not hold for a twin-entry turbine when one of its entries is completely
87 closed. In this case, the flow velocity at the open side is at its maximum value, as expected. The velocity at
88 the other side is not close to zero, but is about the full admission case. At the same time, the flow angle at
89 the closed side increases considerably. Baines and Yeo [4] stated that this velocity increase is due to a
90 sudden expansion. But this conclusion seems to be invalid. Figure 2 shows the radial velocity components at
91 the rotor entry for three different cases. In this figure, the area under the curves indicates the volumetric flow
92 rate. It is clear from the figure that the volumetric flow rate (the area under the curve) when one of the
93 entries is fully closed is not increased, but decreased. So, the statement made in [4] for this phenomenon
94 cannot be justified and the flow is compressed in this case.

95 This behavior can be explained by the following statements. When the mass flow rates at the hub and
96 shroud side entries are different, the flow streams in the interspace affect each other and the flow with higher
97 velocity tends to move the flow at the other side along itself. As the velocity difference between the two
98 entries is increased, the above-mentioned behavior becomes more pronounced due to the friction between
99 two streams and the low momentum of the flow with smaller velocity. At the same time, because of the mass
100 flow rate limitation, the flow at the side with the lower mass flow rate cannot be moved faster along the
101 radial direction. But at the tangential direction, this limitation does not exist. Thus the tangential component
102 of the velocity is increased in this area. As a result, the absolute flow angle and the velocity are increased in
103 the closed side. This explanation is used for modeling in this work.

1.6
1.7

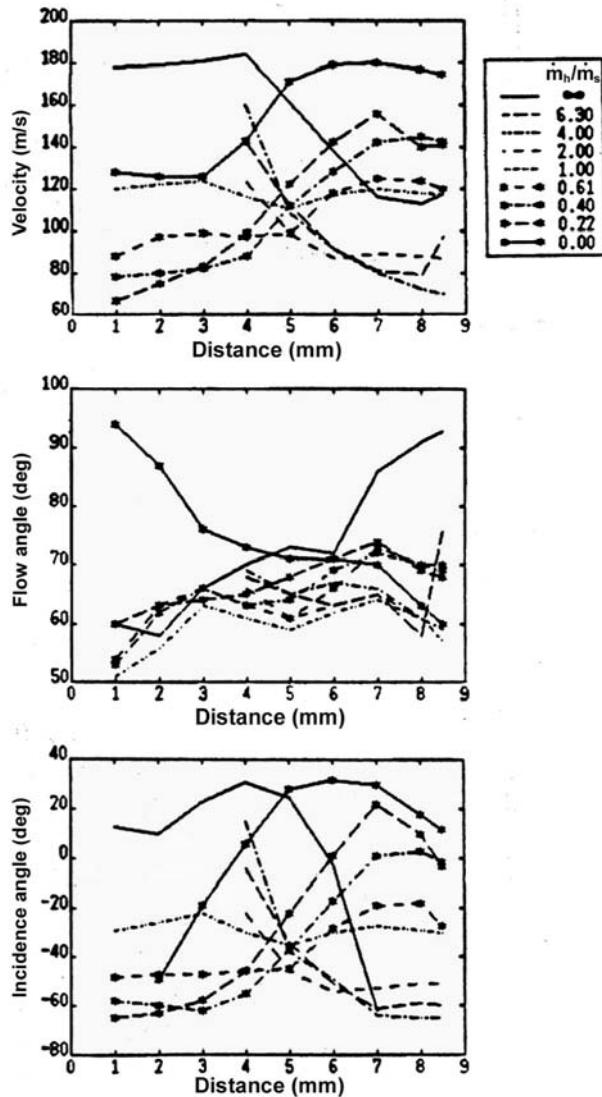


Fig. 1. Flow characteristics at the volute exit from hub side to shroud side [4]

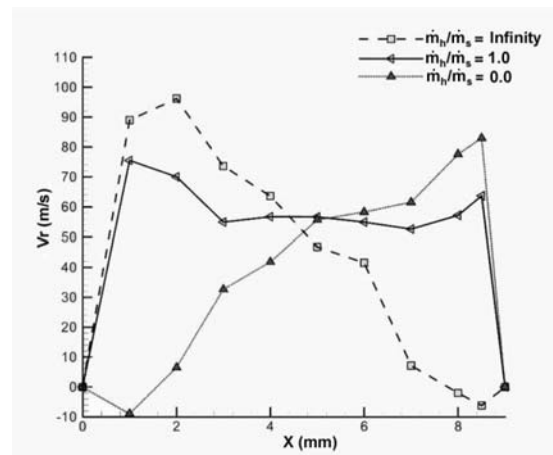


Fig. 2. Radial velocity component at the volute exit from hub side to shroud side

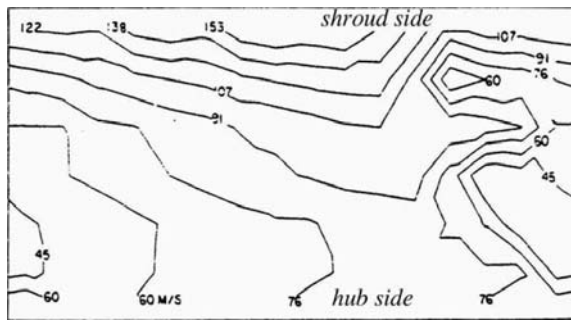
1.8
1.9
1.10

b) Flow in the rotor

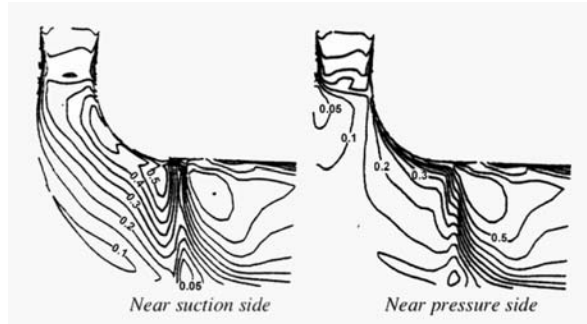
1.11
1.12
1.13
1.14
1.15
1.16
1.17
1.18
1.19
1.20
1.21
1.22

The flow pattern in the rotor affects the characteristics of twin-entry radial turbines. Figure 3 shows the radial component of the flow obtained by laser anemometry at the entrance to the rotor of a single-entry turbine [13]. Figure 4 presents the relative Mach contours in the rotor of a single-entry turbine [14]. As can be seen from these figures, the flow at the rotor entry tends to pass through the region near the shroud. As the flow always passes through the lines that have optimum behavior and minimum losses, in this paper, we have chosen the optimum radial velocity distribution at the entrance to the rotor to be the same as the radial velocity distribution at the rotor entrance of a single-entry turbine with a symmetric volute. So, if the mass flow ratio in the twin-entry turbine entries is such that the radial velocity at the rotor entry is the same as the optimum case, there will not be extra losses in the twin-entry turbine rotor. Otherwise, it is expected to have additional losses in the rotor. Indeed, according to the experimental results [4], the flow pattern at the rotor exit is a weak function of the flow distribution at the rotor entry. In the other hand the flow angle and absolute velocity at the rotor exit under a different partial admission condition is similar to the full admission

123 case. So when the flow pattern at the rotor entry does not match with the optimum case, the flow during a
 124 mixing process along the rotor becomes similar to the optimum condition at the rotor exit. This process
 125 produces additional loss in the rotor, which we call *rotor mixing* loss. Another case which is worth
 126 mentioning, is the effect of the tangential velocity component on the losses. When the tangential velocity at
 127 the rotor entry is different from its optimum value, the incidence losses occur.



128 Fig. 3. Radial velocity contours at the entrance to
 129 the rotor of a single entry turbine [13]



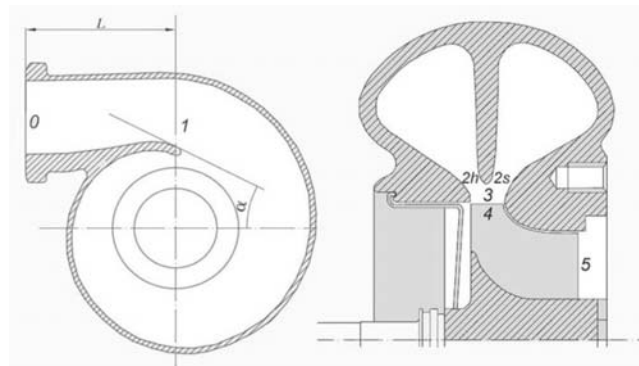
130 Fig. 4. Relative Mach contours in the rotor of a
 131 single-entry turbine [14]

132 In the twin-entry turbines, according to above discussions, it is expected that the higher efficiency can
 133 be obtained when the mass flow rate at the shroud side entry is more than the other side and the minimum
 134 efficiency is obtained when the radial velocity distribution at the rotor entry has the maximum deficiency
 135 with respect to the optimum case. That occurs when the shroud side entry is fully closed.

136 3. MODELING

137 a) One-dimensional equations

138 In one-dimensional modeling, the flow passage is divided into several regions, as shown in Fig. 5, and the
 139 flow is modeled in each part separately. The following equations are used for the flow modeling at the
 140 single-entry turbine rotor [11].
 141



142 Fig. 5. Flow configuration in a twin-entry turbine
 143

$$144 \frac{\dot{m} \sqrt{RT'_{0i}} / \gamma}{A_e P'_{0i}} = \sigma \cdot \cos(\beta_e) M'_e \times \left(1 + \frac{(\gamma-1)}{2} M'^2_e \right)^{\frac{-(\gamma+1)}{2(\gamma-1)}} \left(1 - \frac{U_i^2 - U_e^2}{2c_p T'_{0i}} \right)^{\frac{(\gamma+1)}{2(\gamma-1)}} \quad (1)$$

145 where

$$146 \sigma = e^{(-\Delta s/R)} = \left(1 - \frac{(\gamma-1)}{\gamma} \frac{U_i^2}{RT'_{0e}} \Delta q \right)^{\gamma/(\gamma-1)} \quad (2)$$

$$147 \Delta q = \frac{h'_{0e} - h'_{0es}}{U_i^2} = \frac{\Delta h'_{0es}}{U_i^2} \quad (3)$$

$$h'_0 = h + \frac{1}{2}W^2, \quad T'_0 = h'_0/c_p, \quad P'_0 = P \left(\frac{T'_0}{T} \right)^{\frac{\gamma}{\gamma-1}}, \quad M' = W/a \quad (4)$$

Equation (1) is the non-dimensional mass flow rate equation for the moving passages (rotor). In Eq. (3), Δq is the non-dimensional energy loss in the rotor. Obviously Eq. (1) can only be used for a single-entry turbine. In this paper, this equation is modified for a twin-entry turbine. The derivation of the new formula is given in [15], which leads to

$$\frac{\dot{m}}{A_5} \sqrt{\frac{R}{\gamma}} \cdot \left(\frac{\sqrt{T'_{04,s}}}{P'_{04,s}} \right)^{Mr_s} \cdot \left(\frac{\sqrt{T'_{04,h}}}{P'_{04,h}} \right)^{Mr_h} = \sigma \cdot \cos(\beta_5) M'_5 \times \left(1 + \frac{\gamma-1}{2} M'^2_5 \right)^{\frac{-(\gamma+1)}{2(\gamma-1)}} \times \left\{ \left(1 - \frac{U_4^2 - U_5^2}{2c_p T'_{04,h}} \right)^{Mr_h} \left(1 - \frac{U_4^2 - U_5^2}{2c_p T'_{04,s}} \right)^{Mr_s} \right\}^{\frac{(\gamma+1)}{2(\gamma-1)}} \quad (5)$$

$$\sigma = \sigma_s^{Mr_s} \sigma_h^{Mr_h} \quad (6)$$

$$Mr_s = \frac{\dot{m}_s}{\dot{m}_s + \dot{m}_h}, \quad Mr_h = \frac{\dot{m}_h}{\dot{m}_s + \dot{m}_h} \quad (7)$$

The loss coefficient, σ , depends on the hub and shroud side flow losses. Due to the complexity of the flow in the rotor, it is not feasible to calculate σ_s and σ_h separately. Therefore, the following model, which is obtained by combining Eqs. (2) and (7), is suggested here.

$$\sigma = \left\{ \left(1 - \frac{\gamma-1}{\gamma RT'_{05}} U_t^2 \Delta q_s \right)^{Mr_s} \left(1 - \frac{\gamma-1}{\gamma RT'_{05}} U_t^2 \Delta q_h \right)^{Mr_h} \right\}^{\frac{\gamma}{\gamma-1}} \quad (8)$$

This relation can be simplified by using Taylor series expansion, and then assuming that $(\gamma-1/\gamma RT'_{05}) \times U_t^2 \Delta q$ is small. This assumption is reasonable for a turbine with acceptable performance. The result is

$$\sigma = \left\{ 1 - \frac{\gamma-1}{\gamma RT'_{05}} U_t^2 (Mr_s \Delta q_s + Mr_h \Delta q_h) \right\}^{\frac{\gamma}{\gamma-1}} \quad (8)$$

The above relation means that one can consider the effect of shroud and hub side flow losses in one relation, that is, we estimate Δq_s and Δq_h altogether. So, we can modify the correlations for the loss coefficient in single-entry turbines, to obtain losses in twin-entry turbines.

b) Friction losses

These losses are computed in the same way as the friction losses in a curved passage.

$$\Delta h'_{0s,Fr} = f_c \frac{L_H}{D_H} \frac{\bar{W}^2}{2} \quad (9)$$

where f_c is the skin friction coefficient in curved pipes and is obtained by Schlichting [16], and \bar{W} is the average relative velocity in the passage. They are obtained as follows:

$$f_c = f \left[1 + 0.075 \text{Re}^{0.25} \sqrt{\frac{D_H}{2r_c}} \right] \quad (10)$$

and

$$\bar{W}^2 = \frac{1}{2} \left[(Mr_s W_{4s} + Mr_h W_{4h})^2 + W_s^2 \right]$$

where L_H , D_H , and r_c are hydraulic length and diameter, and mean radius of the passage, respectively. f is the skin friction coefficient for smooth-walled straight pipes.

193 **c) Blade loading losses**
194

195 According to Rodgers [12], the following correlation is used to calculate the blade loading losses.
196

$$197 \Delta h'_{0s,BL} = \frac{V_{r3}^2 D_t}{ZL_R} \quad (11)$$

$$198 V_{i3} = (Mr_s V_{i3,s} + Mr_h V_{i3,h}) \quad (12)$$

199 **d) Clearance losses**
200

201 The clearance losses are calculated from the correlation given by Rodgers [12].
202

$$203 \Delta h'_{0s,Cl} = 0.4(e_{cl}/b_3)V_{i3}^2 \quad (13)$$

204 where V_{i3} is obtained from Eq. (12).
205

206 **e) Rotor mixing losses**
207

208 These extra losses exist only in twin-entry turbines and are due to the mixing of the flow in the rotor
209 when the mass flow ratio of the shroud and hub side entries is different from its optimum value. The
210 optimum condition is defined as the condition in which the radial velocity distribution at the rotor entry is
211 the same as the radial velocity distribution at the rotor entry of a single-entry turbine with symmetric value.
212 This radial velocity distribution is studied and modeled using the experimental result shown in Fig. 3. The
213 model, which is introduced here for estimating the radial velocity component, V_{r3} , at the rotor entry is
214
215

$$216 r^m V_{r3} = Const \quad (14)$$

217
218 If the m is chosen between 0.41 and 0.56, Eq. (13) matches very well with the experimental data in a
219 large portion of blade to blade space, as shown in Figs. 6 and 7. In order to make our model more precise
220 and to make sure that it works in more general cases, ideal flow in a two-dimensional curved passage is
221 numerically simulated and our model is tested and compared with the numerical results. Figure 8 shows the
222 curved passage and Figs. 9 and 10 show the results. As can be shown from the figures, the model with
223 suitable m , which is between 0.47 and 0.5, for wide rang of curvature radius, matches very well with the
224 numerical data. From the above results, the value of m can be obtained by curve fitting. The result is
225

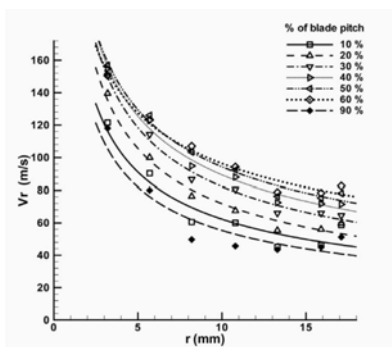
$$226 m = \frac{r_0}{2r_0 + 0.0348b_3} \quad (15)$$

227 For the rotor of a radial flow turbine, the value of r_0 can be calculated from the following formula.
228

$$229 r_0 = B^2/A - b_3/2 \quad (16)$$

230 where

$$231 A = L_R - b_3/2, B = r_t - \sqrt{\frac{r_{5,s}^2 + r_{5,h}^2}{2}}$$



232
233
234
235
236
237
238
239
240
241
242
243
244
245
246
247
248
249
250
251
252
253
254
255
256
257
258
259
260
261
262
263
264
265
266
267
268
269
270
271
272
273
274
275
276
277
278
279
280
281
282
283
284
285
286
287
288
289
290
291
292
293
294
295
296
297
298
299
300
301
302
303
304
305
306
307
308
309
310
311
312
313
314
315
316
317
318
319
320
321
322
323
324
325
326
327
328
329
330
331
332
333
334
335
336
337
338
339
340
341
342
343
344
345
346
347
348
349
350
351
352
353
354
355
356
357
358
359
360
361
362
363
364
365
366
367
368
369
370
371
372
373
374
375
376
377
378
379
380
381
382
383
384
385
386
387
388
389
390
391
392
393
394
395
396
397
398
399
400
401
402
403
404
405
406
407
408
409
410
411
412
413
414
415
416
417
418
419
420
421
422
423
424
425
426
427
428
429
430
431
432
433
434
435
436
437
438
439
440
441
442
443
444
445
446
447
448
449
450
451
452
453
454
455
456
457
458
459
460
461
462
463
464
465
466
467
468
469
470
471
472
473
474
475
476
477
478
479
480
481
482
483
484
485
486
487
488
489
490
491
492
493
494
495
496
497
498
499
500
501
502
503
504
505
506
507
508
509
510
511
512
513
514
515
516
517
518
519
520
521
522
523
524
525
526
527
528
529
530
531
532
533
534
535
536
537
538
539
540
541
542
543
544
545
546
547
548
549
550
551
552
553
554
555
556
557
558
559
560
561
562
563
564
565
566
567
568
569
570
571
572
573
574
575
576
577
578
579
580
581
582
583
584
585
586
587
588
589
590
591
592
593
594
595
596
597
598
599
600
601
602
603
604
605
606
607
608
609
610
611
612
613
614
615
616
617
618
619
620
621
622
623
624
625
626
627
628
629
630
631
632
633
634
635
636
637
638
639
640
641
642
643
644
645
646
647
648
649
650
651
652
653
654
655
656
657
658
659
660
661
662
663
664
665
666
667
668
669
670
671
672
673
674
675
676
677
678
679
680
681
682
683
684
685
686
687
688
689
690
691
692
693
694
695
696
697
698
699
700
701
702
703
704
705
706
707
708
709
710
711
712
713
714
715
716
717
718
719
720
721
722
723
724
725
726
727
728
729
730
731
732
733
734
735
736
737
738
739
740
741
742
743
744
745
746
747
748
749
750
751
752
753
754
755
756
757
758
759
760
761
762
763
764
765
766
767
768
769
770
771
772
773
774
775
776
777
778
779
780
781
782
783
784
785
786
787
788
789
790
791
792
793
794
795
796
797
798
799
800
801
802
803
804
805
806
807
808
809
810
811
812
813
814
815
816
817
818
819
820
821
822
823
824
825
826
827
828
829
830
831
832
833
834
835
836
837
838
839
840
841
842
843
844
845
846
847
848
849
850
851
852
853
854
855
856
857
858
859
860
861
862
863
864
865
866
867
868
869
870
871
872
873
874
875
876
877
878
879
880
881
882
883
884
885
886
887
888
889
890
891
892
893
894
895
896
897
898
899
900
901
902
903
904
905
906
907
908
909
910
911
912
913
914
915
916
917
918
919
920
921
922
923
924
925
926
927
928
929
930
931
932
933
934
935
936
937
938
939
940
941
942
943
944
945
946
947
948
949
950
951
952
953
954
955
956
957
958
959
960
961
962
963
964
965
966
967
968
969
970
971
972
973
974
975
976
977
978
979
980
981
982
983
984
985
986
987
988
989
990
991
992
993
994
995
996
997
998
999
1000

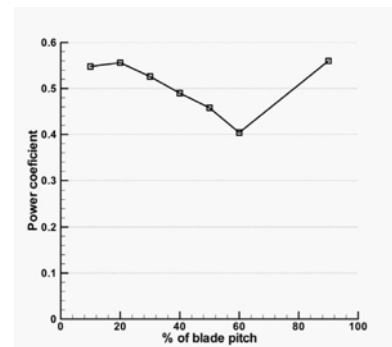


Fig. 7. Values of m for Fig. 6

۲۴۳
۲۴۴
۲۴۵
۲۴۶
۲۴۷
۲۴۸
۲۴۹
۲۵۰
۲۵۱
۲۵۲
۲۵۳

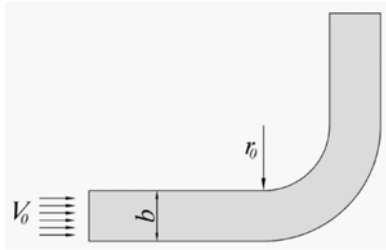


Fig. 8. Simple curved passage

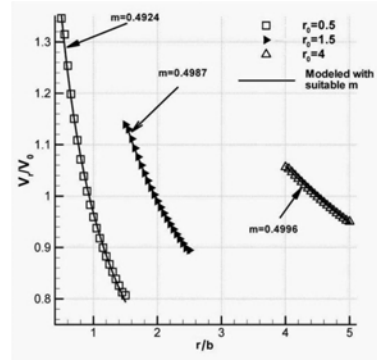


Fig. 9. Radial velocity distribution at the entrance to the passage in Fig. 8

۲۵۴

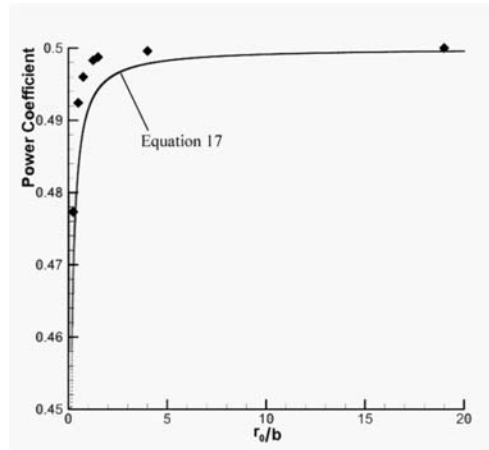


Fig. 10. Value of m for Fig. 9

۲۵۵

۲۵۶

For a twin-entry turbine, the optimum one-dimensional velocity distribution at the rotor entry is assumed as shown in Fig.11. This distribution of the velocity is simplified and a one-dimensional form of Eq. 17.

۲۵۷

۲۵۸

۲۵۹

In order to calculate the rotor-mixing losses, the mixing procedure shown in Fig. 12 has been considered. In this figure, the actual radial velocity distribution at the rotor entry in a particular mass flow ratio and its optimum value, which is obtained after a hypothetical mixing, are shown at sections 1 and 2, respectively. The entropy increase for this process, Δs , can be obtained using one-dimensional thermodynamic relations. So, σ_{RM} is obtained by

۲۶۰

۲۶۱

۲۶۲

۲۶۳

۲۶۴

$$\sigma_{RM} = e^{(-\Delta s_{RM}/R)} \quad (17)$$

۲۶۵

۲۶۶

۲۶۷

As shown in Fig. 12, Δs is estimated from the mixing of the flow in a straight passage. Because the aim of this work is one-dimensional modeling, a straight passage is used rather than a curved passage which corresponds to 2-D or 3-D flows. The optimum condition for the flow leaving a straight passage is a uniform flow. So the modeling for the mixing process is performed by using Fig. 13b. That is, the flow pattern in Fig. 12 is changed to Fig. 13b. This method gives a crude estimation of Δs . Finally, the rotor loss coefficient is obtained by the following relations

۲۶۸

۲۶۹

۲۷۰

۲۷۱

۲۷۲

۲۷۳

۲۷۴

$$\sigma_{rotor} = \sigma_{4-5} = \sigma \cdot \sigma_{RM} \quad (18)$$

۲۷۵

where

۲۷۶

$$\sigma = \left(1 - \frac{\gamma - 1}{\gamma RT_{05}'} U_i'^2 \Delta q \right)^{\frac{\gamma}{\gamma - 1}}, \quad \Delta q = \Delta h'_{0s} / U_i'^2, \quad \Delta h'_{0s} = \sum \Delta h'_{0s} = \Delta h'_{0s,Fr} + \Delta h'_{0s,Cl} + \Delta h'_{0s,BL} \quad (19)$$

۲۷۷
۲۷۸
۲۷۹
۲۸۰
۲۸۱
۲۸۲
۲۸۳
۲۸۴
۲۸۵
۲۸۶
۲۸۷
۲۸۸
۲۸۹
۲۹۰
۲۹۱
۲۹۲

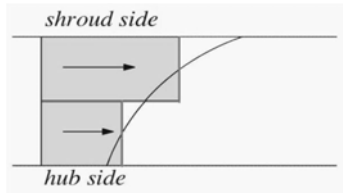


Fig. 11. One-dimensional velocity at the rotor entry

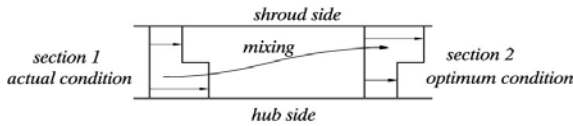


Fig. 12. Mixing process in a hypothetical passage

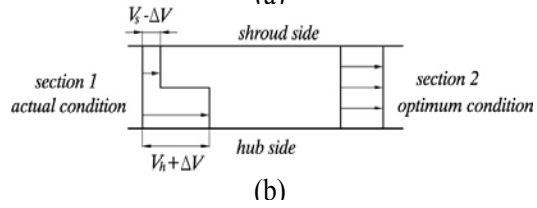
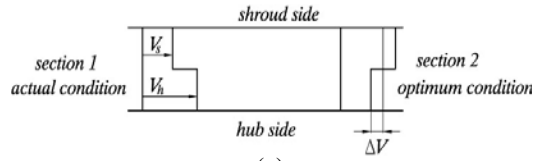


Fig. 13. Modification of the flow pattern leaves the passage shown in Fig. 12 for 1-D modeling

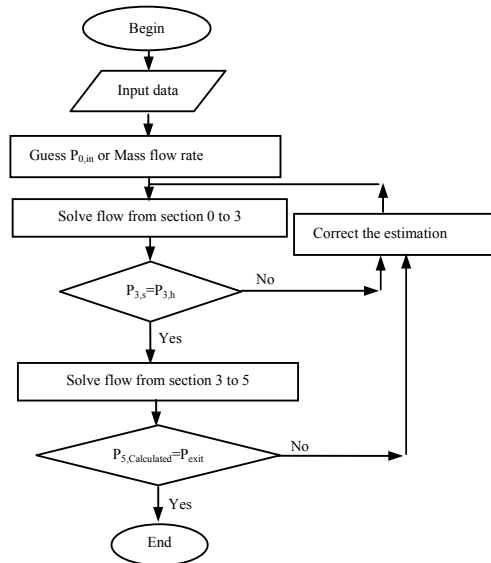


Fig. 14. Solution procedure

۲۹۳
۲۹۴
۲۹۵
۲۹۶
۲۹۷
۲۹۸
۲۹۹
۳۰۰
۳۰۱
۳۰۲
۳۰۳
۳۰۴
۳۰۵
۳۰۶
۳۰۷
۳۰۸
۳۰۹
۳۱۰
۳۱۱
۳۱۲
۳۱۳
۳۱۴
۳۱۵
۳۱۶

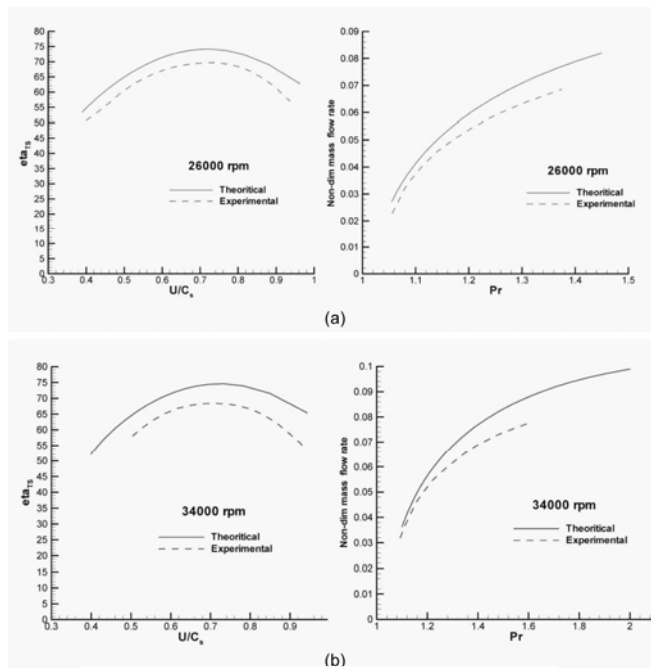


Fig. 15. Full admission results

4. SOLUTION PROCEDURE

As shown in Fig. 5, the flow passages can be divided into several parts. Flow at sections 0 to 2 is considered similar to the single-entry turbine and can be considered as stated in references [7, 8, 10, 11]. For flow between sections 2 and 3, flows in the shroud and hub side are considered separately, but their interactions are considered for calculating the exit flow angles and loss coefficients. Losses due to the friction between two streams are calculated from relations of a mixing layer between two incompressible streams. For the region between sections 3 and 4, the flows in the shroud and hub sides are modeled separately using the NASA incidence loss model [6]. Finally, the flow between sections 4 and 5 is modeled using Eq. (8).

The solution procedure is outlined in the flow chart of Fig. 14. Two types of boundary conditions are used to solve the problem. For the first case, the mass flow rate of each entry is given and for the second case, the total pressure at each entry is identified. More details of the flow solution are given in [15].

5. RESULTS

The results are compared with experimental results presented by Dale and Watson [2] and shown in Figs. 15 and 16. In Figs. 15a and 15b, the mass flow characteristics and the turbine efficiency, at full admission for 26000 rpm and 34000 rpm are shown respectively. As shown in the figures, the calculated efficiency and the mass flow rate are somewhat overestimated, but they are consistent. That is, as the efficiency is overestimated, the losses in the turbine are underestimated, thus the mass flow rate is more than what it should be.

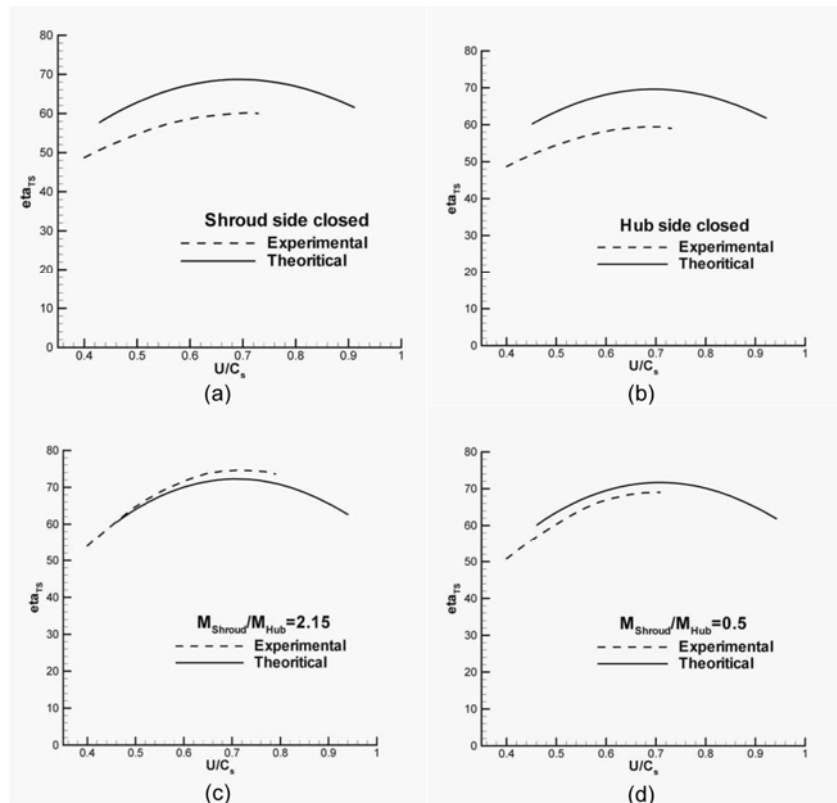


Fig. 16. Partial admission results

Figures 16a to 16d show the efficiency of the turbine at partial admission conditions for 26000 rpm, compared with the experimental data. As shown in the figures, rather good agreements are obtained. Although the trends of the curves are very well matched, there are some differences between the calculated and experimental data. These differences can be due to the following: The uncertainty in the experimental data, especially for high U/C_s , as shown in Fig. 17, gives some inaccurate data. This makes sense especially

because at high U/C_s , more disagreement between the experimental and calculated data is indicated. Secondly as shown in the figures, when the mass flow ratio of the turbine entries is far from its optimum value, the difference between the calculated and experimental results is higher. This matter suggests that the rotor mixing losses are estimated less accurately.

The difference between the efficiencies for two partial admission conditions (where the inflow is either higher in the shroud-side or in the hub-side entry) is due to the effect of the rotor-mixing losses, which are different in the two cases. As shown in Fig. 18 this difference is rather underestimated.

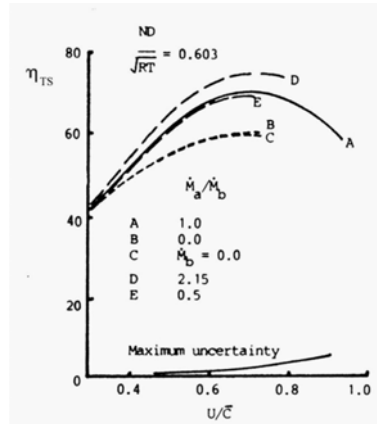


Fig. 17. Experimental results of twin-entry turbine [2]

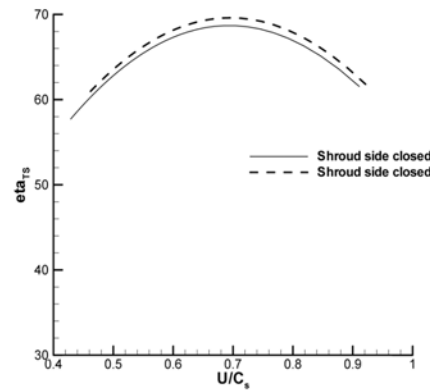


Fig. 18. The difference between the efficiency of the turbine under two partial admission conditions

6. CONCLUSION

In this paper, a one-dimensional performance prediction method is developed for modeling the flow behavior in the twin-entry turbine under partial admission and steady flow conditions. The one-dimensional equations, which are used to analyze the flow in a single-entry turbine, are modified for twin-entry turbine. Also, the rotor mixing losses are added as extra losses. The results are compared with the experimental data [2] and good agreements are obtained. The difference between the results is maybe due to the experimental uncertainty and also underestimating the rotor mixing losses. The agreements are much better when the shroud side and hub side mass flow ratio is close to its optimum value, which corresponds to when the rotor mixing losses are negligible. Because obtaining the loss coefficients in one-dimensional modeling depends on the available experimental data, the model presented here can be improved by using more experimental data.

NOMENCLATURE

A	area	\dot{m}	mass flow rate
a	speed of sound	P	pressure
b	blade height, Passage with	R	gas constant
C_s	isentropic expansion velocity	Re	Reynolds number
D	diameter	r	radius
e	clearance between rotor blades and shroud	r_c	radius of curvature
f	skin friction coefficient for smooth-walled straight pipe	s	entropy
f_c	skin friction coefficient for curved pipe	T	temperature
L	length	U	blade velocity
Mr_h	shroud side entry mass flow rate to total mass flow rate ratio	V	absolute velocity
Mr_s	hub side entry mass flow rate to total mass flow rate ratio	W	relative flow velocity
		Z	rotor blade numbers
		β	relative angle of flow
		γ	specific heat ratio

η	efficiency	h	hub side
σ	loss coefficient	H	hydraulic
Subscripts		i	passage inlet
0	turbine entry, Stagnation properties	RM	rotor mixing
0-5	locations within turbine (see Fig.5)	R	rotor
BL	blade loading	r	radial direction
Cl	clearance	s	isentropic process, Shroud side
E	passage exit	TS	total to static
Fr	friction	t	blade tip, Tangential direction

REFERENCES

1. Pischinger, F. & Wunsche, A. (1977). The characteristic behaviour of radial turbines and its influence on the turbocharging process. *MAC Conference*, Tokyo.
2. Dale, A. & Watson, N. (1986). Vaneless radial turbocharger turbine performance. *IMEchE Conference Paper C110/86 in Turbocharging and Turbochargers*.
3. Capobianco, M. & Gambarotta, A. (1993). Performance of a twin-entry automotive turbocharger turbine. ASME Paper 93-ICE-2.
4. Baines, N. C. & Yeo, J. H. (1991). Flow in a radial turbine under equal and partial admission conditions. IMechE Paper C423/002.
5. Lymberopoulos, N., Baines, N. C. & Watson, N. (1988). Flow in single and twin entry turbine volutes. ASME Paper 88-GT-59.
6. Futral, S. M. & Wasserbauer, A. C. (1965). Off-design performance prediction with experimental verification for a radial-inflow turbine. NASA TN D-262.
7. Wallace, F. J., Baines, N. C. & Whitfield, A. (1976). A unified approach to the one-dimensional analysis and design of radial and mixed flow turbines. ASME paper 76-GT-100.
8. Abidat, M., Hachemi, M. K. & Baines, N. C. (1988). Prediction of the steady and non-steady flow performance of a highly loaded mixed flow turbine. *Proceedings of Institution of Mechanical Engineers, Part A: Journal of Power and Energy*, 212, 173-184.
9. Chen, H. & Baines, N. C. (1994). The aerodynamic loading of radial and mixed-flow turbines. *International Journal of Mechanical Science*, 36, 63-79.
10. Whitfield, A. & Baines, N. C. (1976). A general computer solution for radial and mixed-flow turbomachine performance prediction. *International Journal of Mechanical Science*, 18, 179-184.
11. Whitfield, A. & Baines, N. C. (1990). *Design of radial turbomachines*, Longman Scientific & Technical.
12. Rodgers, C. (1987). Mainline performance prediction of radial inflow turbines. VKI Lecture series 1987-07.
13. Benisek, E. F. & Struble, A. G. (1990). Laser velocity measurements in a turbocharger turbine. *IMEchE paper C405/009*.
14. Zangeneh-Kazemi, M., Dawes, W. N. & Hawthorne, W. R. (1988). Three dimensional flow in radial-inflow turbines. ASME Paper 88-GT-103.
15. Ghassemi, Sh. (2001). Experimental and theoretical investigation of twin-entry turbine behavior. Mechanical Engineering Department, Isfahan University of Technology, Isfahan, Iran, M.Sc. Thesis in Farsi.
16. Schlichting, H. (1968). Translated by Kestin, J., *Boundary-layer theory*, Sixth edition, McGraw-Hill Book Company.

